

# Development of an Advanced Motor Control System for Electric Vehicles

## Abstract

Electric vehicles are considered as one of the most popular way to decrease the consumption of petroleum resources and reduce environmental pollutions. Motor control system is one of the most important part of electric vehicles. It includes power supply module, IGBT driver, digital signal processing (DSP) controller, protection adjustment module, and resolver to digital convertor. To implement the control strategies on motor control system, a lot of practical aspects need to be taken into accounts. It includes setup of the initial excitation current, consistency of current between motor and program code, over-modulation, field weakening control, current protection, and so on. In this paper, an induction motor control system for electric vehicles is developed based on DSP. The control strategy is based on the field-oriented control (FOC) and space vector pulse width modulation (SVPWM). Speed calculation, over-modulation, field weakening control, PI controller, and fault diagnosis are also applied in this DSP algorithm. As an industry product running on a real electric bus with a 100kW induction motor, communication with vehicle control unit (VCU) by CAN bus, control system safety and PC software designed for lab experiments are also discussed. This paper focused on how to develop the advanced motor control system for electric vehicles for industrial application. The steady-state and transient performances of this motor control system are analyzed by both test-bench experiments and road experiments. Its performance is satisfactory when applied to the real electric vehicle.

## Introduction

Recently, electric vehicles have been promoted as a practical platform for reducing environmental pollution and mitigating energy crisis. Vehicle control unit (VCU), motor control system (MCU), and battery management system (BMS) are the main control systems of electric vehicles. Other technologies of electric vehicle include the motor design, body and chassis design, battery design, and particularly the system-level design and optimization of electric motor drive systems [1, 2, 3].

Motor control system plays a very important role in driver safety and comfort. Induction motors (IMs) are widely used for electric vehicles due to their simple structure, good performance, and low cost [4, 5, 6]. As for the control methods for IM, there are the V/F control, field oriented control (FOC), direct torque control (DTC) and some modern control methods, like model predictive control (MPC), fuzzy control, and neural networks. However, for industrial products of electric vehicles, FOC appears to be the most popular control strategy [7, 8].

This paper is focused on how to develop the induction motor advanced control system for electric vehicles based on DSP. Apart from the implementation of FOC and SVPWM, some practical problems, such as current protection, over-modulation and field weakening control method are all discussed and the performance of final control strategy is verified on a real electric bus. This paper shows some aspects, which need to be taken into account when developing motor control methods on digital control chips, like DSP, for industrial application. It will do some help for applying new control methods like MPC on industrial motor to achieve better performance.

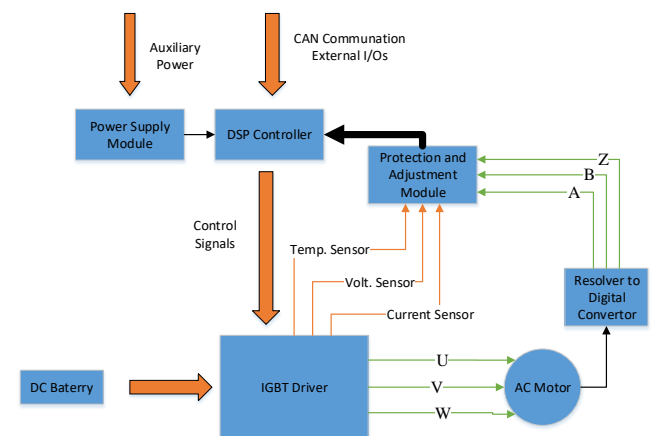


Figure 1. Diagram of motor control system.

## Construction of Motor Control System

### Basic Diagram of the System

Figure 1 shows the diagram of the motor control system. The motor control system of electric vehicle includes the power supply module, IGBT driver, DSP controller, protection and adjustment module, and resolver to digital convertor. The power source of this electric bus is a 650V battery set. It supplies voltage to IGBT driver and converts it to various voltage power source as required for other parts of motor control system. IGBT module receives instructions from DSP controller and produces balanced three phase voltage (U V W) to drive the induction motor. It also collects the temperature, voltage and current signals and then transfers them to the DSP controller via protection and adjustment module. Resolver to digital convertor detects the motor speed with direction and then produces three corresponding signals (A B Z) and transfers them to DSP for speed



Giving  $U_\alpha$  and  $U_\beta$ , one can have a  $U_{ref}$  as input, which can be equally obtained from two of the six basic vectors. In the DSP program, it is needed to acquire the PWM durations  $T_1$  and  $T_2$  of the two corresponding basic vectors. Therefore, one has to know in which sector the  $U_{ref}$  is located for acquiring the correct duration. To find out the correct sector, three variables,  $V_{ref1}$ ,  $V_{ref2}$ ,  $V_{ref3}$  are used.

$$V_{ref1} = U_\beta \quad (1)$$

$$V_{ref2} = \frac{-U_\beta + \sqrt{3}U_\alpha}{2} \quad (2)$$

$$V_{ref3} = \frac{-U_\beta - \sqrt{3}U_\alpha}{2} \quad (3)$$

If  $V_{ref1} > 0$  then  $a=1$ , else  $a=0$ . If  $V_{ref2} > 0$  then  $b=1$ , else  $b=0$ . If  $V_{ref3} > 0$  then  $c=1$ , else  $c=0$ ;

The sector is defined as,  $sector=4*c+2*b+a$ . According to this, the correct sector, in which the  $U_{ref}$  is located, can be worked out. As to the duration, it can be found out that there are only three basic values for calculating in all the possible occasions. Variables  $X$ ,  $Y$ ,  $Z$  are used here to calculate the final duration, where

$$X = U_\beta \quad (4)$$

$$Y = \frac{1}{2}(\sqrt{3}U_\alpha + U_\beta) \quad (5)$$

$$Z = \frac{1}{2}(-\sqrt{3}U_\alpha + U_\beta) \quad (6)$$

Then the duration table can be obtained as table 1 shows. As implementation is based on DSP, one should use the related registers to get the trigger value and thus one can get the expected PWM for motor drive [7].

QEP MACRO and SPEED FR MACRO are the parts of calculation of motor speed. CURMOD MACRO is the current module. It uses the motor speed to calculate the electrical angle, which is needed for Park transformation and inverse Park transformation. PID MACRO is the PID control unit. It plays a great role in the transient and steady-state performance of the control system.

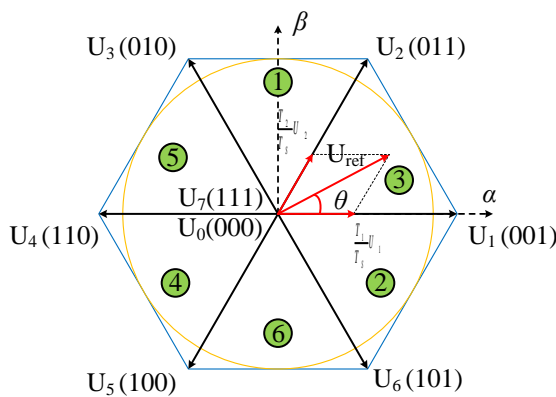


Figure 3. SVPWM scheme:  $U_1$ - $U_6$  are the basic vectors,  $U_0$  and  $U_7$  are the zero vectors, and  $T_s$  is the control period.

Table 1. Duration select table

| Sector | 3         | 1         | 5         | 4         | 6         | 2         |
|--------|-----------|-----------|-----------|-----------|-----------|-----------|
| Vector | U1,<br>U2 | U3,<br>U2 | U3,<br>U4 | U5,<br>U4 | U5,<br>U6 | U1,<br>U6 |
| t1     | -Z        | Z         | X         | -X        | -Y        | Y         |
| t2     | X         | Y         | -Y        | Z         | -Z        | -X        |

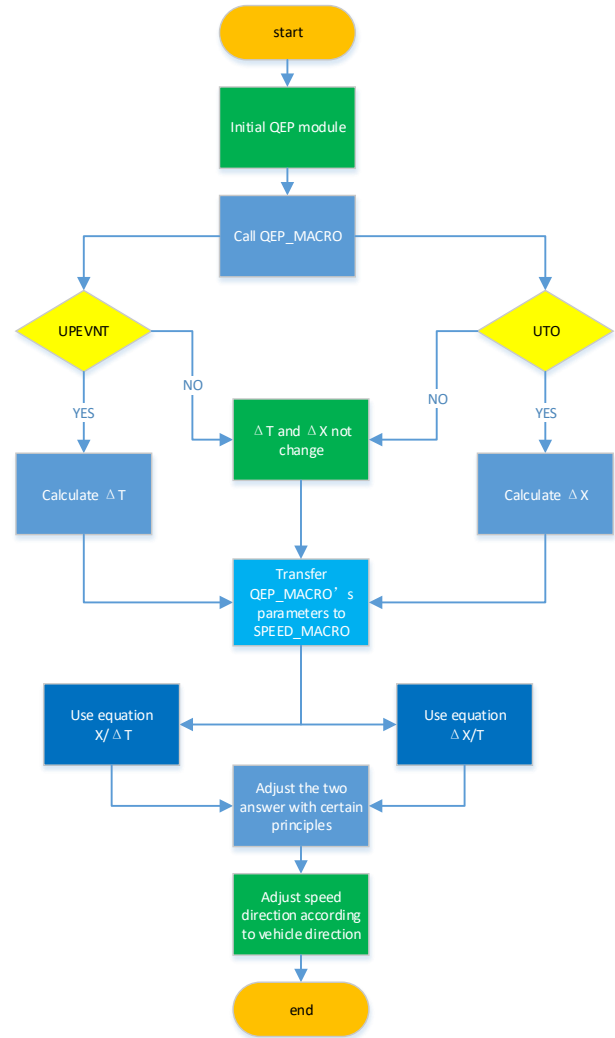


Figure 4. Speed calculation flow diagram

### Speed Calculation Algorithm

Speed measurement is a very important value for the FOC algorithm. The current module needs the value of speed to estimate the flux angle while Park transformation and Clark transformation need the

flux angle to do calculation. The speed measurement equations are shown as (7) and (8).

$$v_L(k) = \frac{x}{t(k)-t(k-1)} = \frac{x}{\Delta T} \quad (7)$$

$$v_H(k) = \frac{x(k)-x(k-1)}{T} = \frac{\Delta X}{T} \quad (8)$$

where

X: Unit position defined by integer multiple of quadrature edges

ΔT: Elapsed time between unit position events

Δx: Incremental position movement in unit time

T: Unit time

Equation (7) is used for low speed measurement and equation (8) is for high speed measurement. Final speed used in algorithm is derived from a combination of this two methods. Speed calculation flow is shown as figure 4.

### DSP Algorithm

The FOC is implemented on DSP and it is the major part of the motor control system for electric vehicle. Its control frequency is actually based on the PWM interrupt service frequency. In addition to the main FOC algorithm, over-modulation, field weakening control, the system protection, error detection, communication with PC and vehicle control unit, and other aspects, are also considered [12].

The main program flow diagram is shown in Figure 5. When the motor control system starts, the system clock and GPIO are initialized by function DeviceInit(). MemCopy() moves MainISR to RAM from flash to save running time. GetSysPara() is the function of reading parameters from FRAM, which is based on protocol I<sup>2</sup>C. These parameters include the motor parameters and some parameters for communication between DSP and PC. Three tasks are always running in the background loop. The FOC control algorithm runs in PWM interruption service function program (PWM\_ISR) and FAULT\_ISR deals with all the error diagnose work. When the system detects some errors in running state, the protection action will be triggered and the motor speed will decelerate gradually and then the motor will shut down in the end. Errors will be uploaded to the vehicle control unit or PC for further analysis. The PWMISR program flow diagram is shown in Figure 6. The modules mentioned in the FOC scheme are used in this program. PWM signals are produced as required by these program.

As this development is based on DSP and used for electric vehicles, some work about electric vehicle also needs to be accomplished. Three tasks in background loop are used to deal with the following problems. AD sampling, temperature and battery voltage monitor, current protection and collecting data for analysis are running in task A. Communications with PC and vehicle control unit are operating in task B and task C. The CAN module of DSP is used to perform this communication. When transferring data by CAN, the protocol with each terminal equipment needs to be made. The driver's instructions, like starting moving, stopping moving, accelerating the speed, and changing gears, are all sent by CAN in these tasks.

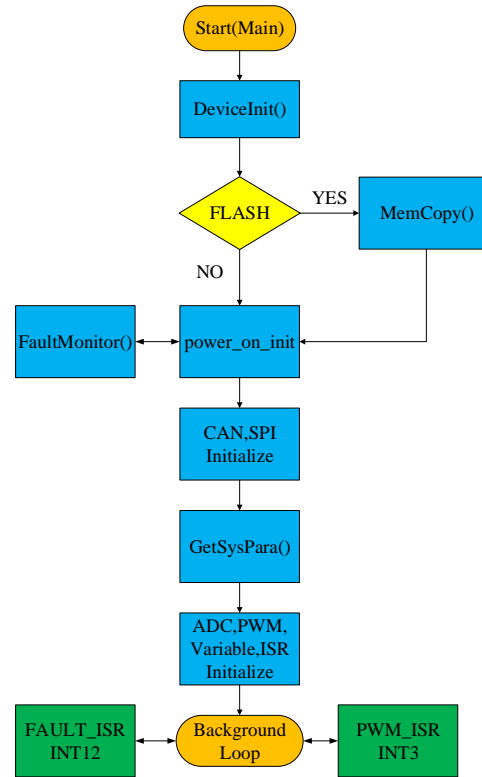


Figure 5. Main DSP program flow diagram.

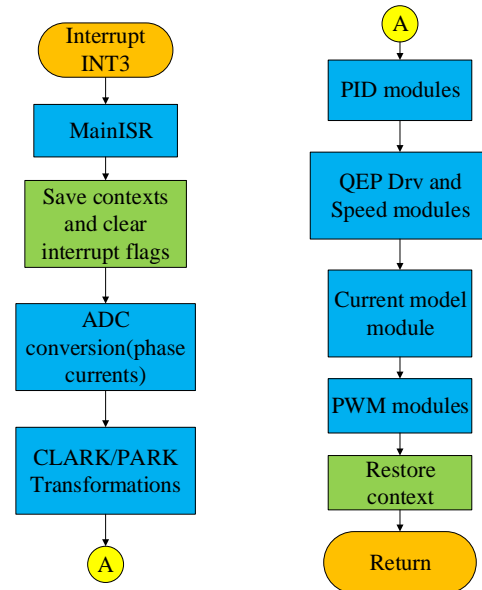


Figure 6. PWMISR program flow diagram

### Practical Problems

The motor control system is designed for real electric vehicle, some practical problems of development need to be considered.

## Initial Excitation Current

The flux is calculated on  $I_{sd}$  and torque is related to  $I_{sq}$ . For convenience,  $I_d$  presents  $I_{sd}$  and  $I_q$  presents  $I_{sq}$  in the flowing part for implementing on electric vehicle.  $I_q$  is an important parameter for the driver's acceleration paddle.  $I_d$  is not controlled by the driver and thus it should be set up as initial value in the program. The no-load current is  $I_0$ , which is a constant of the motor. Therefore, it is requested to decide the correct  $I_d$  from  $I_0$ .

The inverse Park transformation is:

$$\begin{bmatrix} I_\alpha \\ I_\beta \end{bmatrix} = \begin{bmatrix} \cos\theta & -\sin\theta \\ \sin\theta & \cos\theta \end{bmatrix} \begin{bmatrix} I_d \\ I_q \end{bmatrix} \quad (9)$$

Where  $I_d, I_q$  are the currents in rotating coordinates frame and  $I_\alpha, I_\beta$  are the currents in stationary coordinates frame, and  $\theta$  is the electrical angle, respectively.

Set  $I_q = 0$ , one can have

$$I_\alpha = \cos\theta * I_d \quad (10)$$

$$I_\beta = \sin\theta * I_d \quad (11)$$

The Clark transformation is:

$$\begin{bmatrix} I_a \\ I_b \\ I_c \end{bmatrix} = \begin{bmatrix} 1 & 0 \\ -\frac{1}{2} & \frac{\sqrt{3}}{2} \\ -\frac{1}{2} & -\frac{\sqrt{3}}{2} \end{bmatrix} \begin{bmatrix} I_\alpha \\ I_\beta \end{bmatrix} \quad (12)$$

where  $I_a, I_b, I_c$  are the currents in the three phase frame.

Combining (12) with (10) and (11), one can have

$$I_a = \cos\theta * I_d \quad (13)$$

$$I_b = \cos(\theta - 120^\circ) * I_d \quad (14)$$

$$I_c = \cos(\theta + 120^\circ) * I_d \quad (15)$$

The RMS current of  $I_a$  equals  $I_d/\sqrt{2}$ , and thus

$$I_d = \sqrt{2}I_0 \quad (16)$$

According to (16), the correct excitation current can be confirmed for the system based on motor parameters.

## Current Consistency of Program and Motor

In the DSP program, the three phase currents of motor,  $I_a, I_b$  and  $I_c$ , can be used and the program produces duration of PWM to control the current. The motor has three phases, namely, U, V and W. When producing the PWM duration, the correct basic vector is used, which is directly related to the three physical bridges of IGBT. The phase current data are obtained by AD converter. The correct corresponding feedback current is needed to calculate the error as input of PID controller.

Page 5 of 8

12/20/2018

1. Set  $I_d=1$ , and  $I_q=0$ ,  $\theta=0$ , according to inverse Park transformation and Clark transformation, the voltage vector is around  $U_1(001)$ . Check the motor's three phase output, U V W. The phase with longest time of high level means that it is the feedback of  $I_a$  in the program. Figure 7 shows that phase U has the longest high level voltage, so it is connected to phase A in program. Notice that, when doing experiment,  $I_d=0.95$  and  $I_q=0.05$  was set for safety, which doesn't affect the results and conclusions.
2. Set  $I_d=0$ , and  $I_q=1$ , which means that the voltage vector is combination of  $U_3(010)$  and  $U_2(011)$ . Check the output of U V W. The phase with longest time of high level means the feedback of  $I_b$  and that with the shortest time of high level means the feedback of  $I_c$ . Figure 8 shows that phase V has the longest high level voltage, so it is connected to phase B in program. Phase W has the shortest time of high level so it is connected to phase C in program.

According to these experiments,  $I_a, I_b$ , and  $I_c$  in the program can match with the physical motor phases U, V, and W. In this case, motor phase U is connected to program phase A, V is connected to phase B, and W is connected to phase C. As for the hardware, motor phase U is connected to ADC channel 2, V is connected to ADC channel 0, and W is connected to ADC channel 1. So phase A, B, C should use ADC channel 2, 0, 1, separately, for correct physical connection. If they do not match, the performance of torque and speed would be very bad.

## Current Zero Drift Compensation

Before the main algorithm starts, OffsetISR interruption service function runs first. Phase current A, B, C are calculated for 500 times and the average value for each phase current is taken as its offset current separately for compensation in OffsetISR program. Once this job is done, the PWM service entrance changes to mainISR for the main algorithm. Phase current is compensated by the offset current calculated in OffsetISR, so that the current zero drift is fixed.

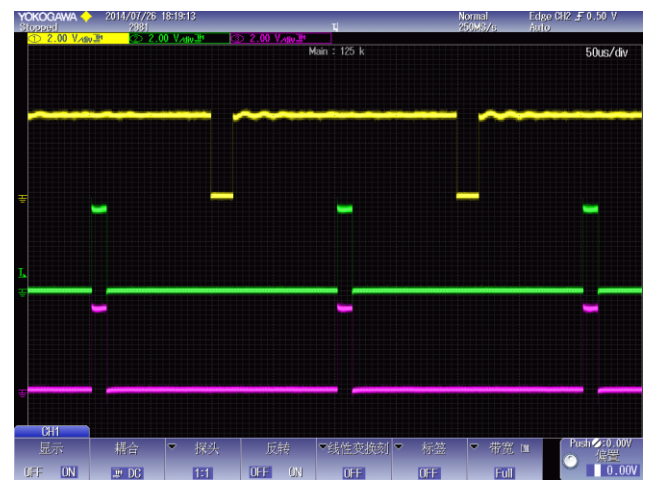


Figure 7.  $I_d=0.95, I_q=0.05$ , yellow signal- phase U, green – phase V, pink - phase W.



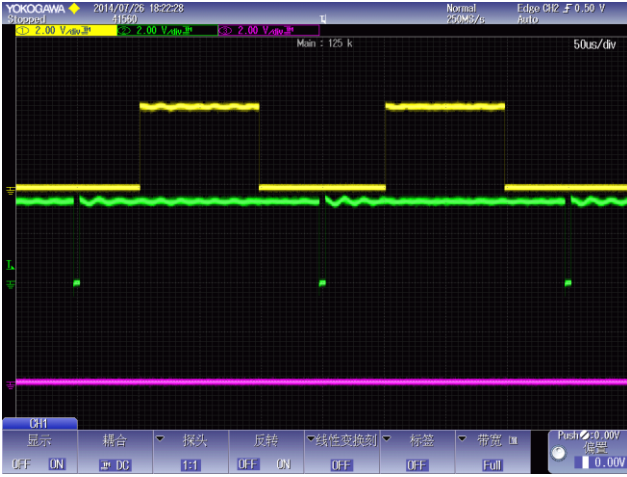


Figure 8.  $I_q=0.95, I_d=0.05$ , yellow signal – phase U, green – phase V, pink – phase W.

### Over Modulation

When the values of  $I_d$  and  $I_q$  are given, the  $U_{ref}$  is settled as well. According to the principle of SVPWM, the duration of PWM as  $T_1$  and  $T_2$  can be obtained. However, improper  $U_{ref}$  could lead to the sum of  $T_1$  and  $T_2$  of more than unit 1. In the program, the unit 1 is settled by control period. Therefore, when  $T_1$  or  $T_2$  is not correct, the distortion of current and low power efficiency may happen. To avoid this situation, an easy but proper way is proposed. That is to scale down  $T_1$  and  $T_2$  to make their sum equal to unit 1. The logic diagram is shown in Figure 9.

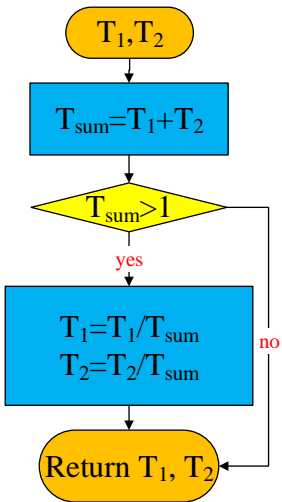


Figure 9. Over-modulation logic diagram

### Field Weakening Control Strategy

The system power will reach its rated value when the motor reaches its rated speed. To achieve higher speed, the excitation current needs to be reduced. In this project, a variable  $x_m$  is used to weaken the flux. It can be written as the form (17) shown, where  $v$  is speed of the motor.

$$x_m = f(v^{-1}, v^{-2}) \quad (17)$$

In this platform,  $x_m$  is chosen as equation (18)

$$x_m = \begin{cases} 0.83 * v^{-1} * v_m & \text{if } v \leq 1.2 * v_m \\ v^{-2} * v_m^2 & \text{if } v > 1.2 * v_m \end{cases} \quad (18)$$

Where  $v_m$  is the rated speed, which equals to 1000rpm in this project.

Figure 10 is a situation when  $x_m$  is not appropriate, which results in speed getting capped and staying in its highest speed after reaching rated speed. Speed can increase well in Figure 11 while  $x_m$  works referring to equation (18). In this two figures, for current variables, Y-axis has a bias of 12735 and the value it shows is ten times the real value of  $I_d, I_q$ , respectively. The speed value is shown as it is. In figure 10, motor speed couldn't increase after it reaches around rated speed while motor speed in figure 11 could, which verifies the importance of field weakening control strategy. A good strategy could lead a better speed range in real electric vehicles.

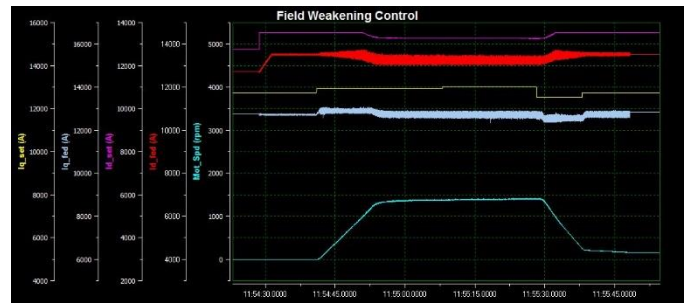


Figure 10. Speed and  $I_d$  responses versus changing  $I_q$  when  $x_m$  is not appropriate

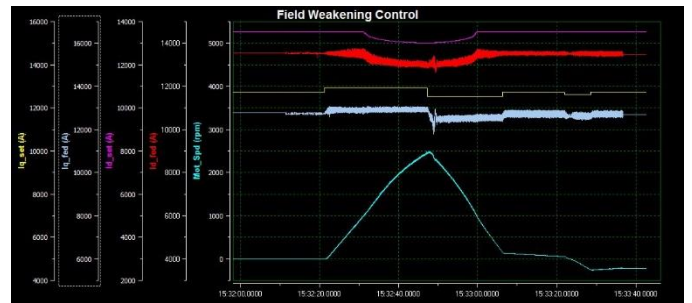


Figure 11. Speed and  $I_d$  responses versus changing  $I_q$  when  $x_m$  is appropriate

### PC Software

A PC software is designed for the experiments of motor control system. It has function of downloading motor parameters to DSP, start running, stop running, monitor of program parameters and some other functions. CAN communication protocol between PC software and DSP is designed as needed.

### Experimental Results and Discussions

Figure 12 shows the experiment setup, with the voltage source, dynamometer, target induction motor, current sensors, oscilloscope, etc. The parameters [13] of target motor is listed in Table 2.

The experiment is carried out on a towing electric motor test bench. When the experiments are conducted for testing speed performance, the opposite motor will offer a fix torque. When the experiments are conducted for torque performance, the opposite motor will offer a fix speed. By doing these, the transient performance and steady state performance can be achieved.

When the electric vehicle driver gives an acceleration signal, it will be finally transferred to an  $I_q$  value by the motor control system and then carried out to obtain a demanded torque and the speed of vehicle increases as a consequence. For experiment at lab, the motor control system can be connected with PC and the instruction is given by software in PC. The load motor can be set to run at a fix speed and then different  $I_q$  is set to acquire the torque performance of target motor. The responses of torque regarding to different input values of  $I_q$ , is shown in Figure 13 and the torque ripples around rated value (1000 Nm) is shown in Figure 14. The voltage and phase current is shown in figure 15 and figure 16. Voltage doesn't change much during change of  $I_q$ . Phase current increases with the increase of  $I_q$  and these three phase current is balanced all the time as Figure 16 shows. In Figure 13,  $I_q$  is increased step by step, while the speed is fixed by the opposite motor as a load. The transient response is satisfactory and its torque is very stable with a ripple of under  $\pm 3\%$ , which is normally considered as a good performance for electric bus.

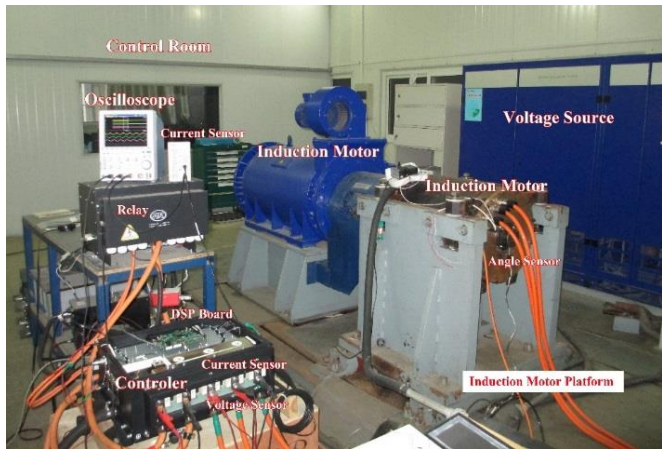


Figure 12. Experiment setup.

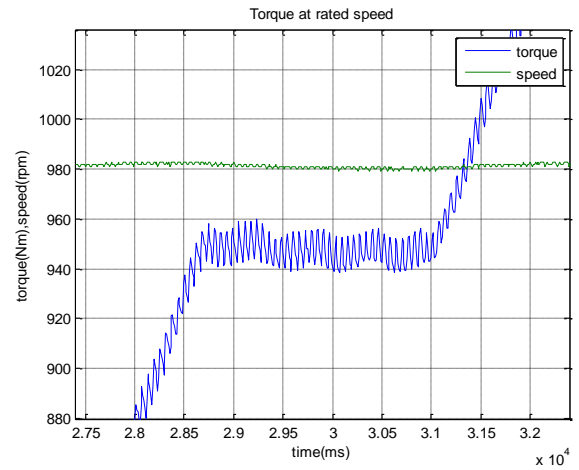


Figure 14. Ripples at rated torque.

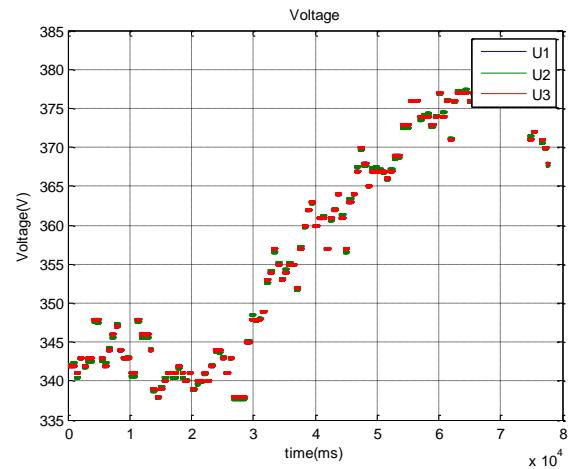


Figure 15. Voltage responses versus changing  $I_q$

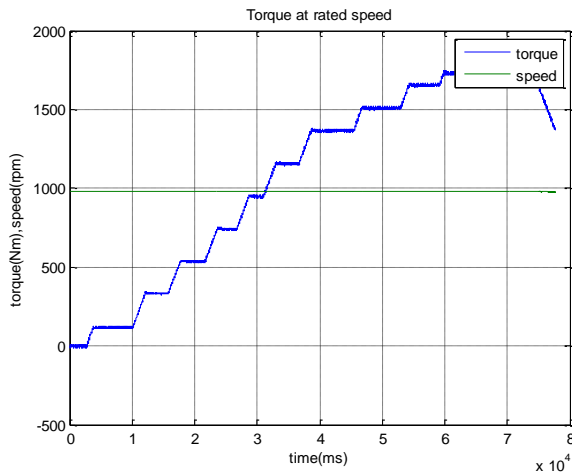


Figure 13. Torque responses versus changing  $I_q$

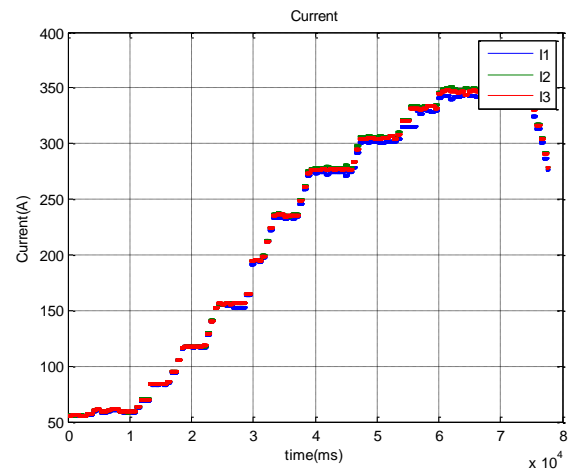


Figure 16. Phase current responses versus changing  $I_q$

Table 2. Motor parameters

| Motor Parameters     | Value | Unit     |
|----------------------|-------|----------|
| Rated power          | 100   | kW       |
| Rated voltage        | 350   | V        |
| Rated current        | 178   | A        |
| Rated speed          | 1000  | rpm      |
| Number of pole pairs | 3     |          |
| Rr                   | 0.01  | $\Omega$ |
| Lr                   | 7.5   | mH       |
| Rs                   | 0.019 | $\Omega$ |
| Ls                   | 10.9  | mH       |
| Peak power           | 250   | kW       |
| Max torque           | 2400  | Nm       |

## Summary

This paper introduces the development of an advanced motor control system for electric vehicles based on DSP. Some problems of development as industrial product are put forward and some corresponding solutions are also proposed. Its torque responds are fast and stable. Its performance is verified by experimental results with a 100 kW induction motor, which are satisfactory. This motor control system is easy to match for different induction motors and thus it can be widely used for electric vehicles.

## References

1. Xu, W., Zhu, J., Guo, Y., Wang, S. et al., "Survey on Electrical Machines in Electrical Vehicles," Paper presented at the 2009 International Conference on Applied Superconductivity and Electromagnetic Devices, ASEMD 2009, September 25, 2009 - September 27, 2009, Chengdu, China, 2009.
2. Lei, G., Wang, T., Guo, Y., Zhu, J. et al., "System-Level Design Optimization Method for Electrical Drive Systems-Robust Approach," *Ieee Transactions on Industrial Electronics* 62, no. 8 (Aug 2015): 4702-13, doi: 10.1109/TIE.2015.2404305
3. Lei, G., Wang, T., Guo, Y., Zhu, J. et al., "System-Level Design Optimization Methods for Electrical Drive Systems: Deterministic Approach," *Ieee Transactions on Industrial*

*Electronics* 61, no. 12 (Dec 2014): 6591-602, doi:10.1109/TIE.2014.2321338

4. Xu, W., Zhu, J., Tan, L., Guo, Y. et al., "Optimal Design of a Linear Induction Motor Applied in Transportation," *2009 Ieee International Conference on Industrial Technology, Vols 1-3* (2009): 318.
5. Guo, Y., Xu, W., Zhu, J., Lu, H. et al., "Design and Analysis of a Linear Induction Motor for a Prototype Hts Maglev Transportation System," Paper presented at the 2009 International Conference on Applied Superconductivity and Electromagnetic Devices, ASEMD 2009, September 25, 2009 - September 27, 2009, Chengdu, China, 2009.
6. Xu, W., Zhu, J., Zhang, Y., Li, Y. et al., "An Improved Equivalent Circuit Model of a Single-Sided Linear Induction Motor," *Ieee Transactions on Vehicular Technology* 59, no. 5 (Jun 2010): 2277-89, doi:10.1109/Tvt.2010.2043862.
7. Casadei, D., Profumo, F., Serra, G., and Tani, A., "Foc and Dtc: Two Viable Schemes for Induction Motors Torque Control," *Ieee Transactions on Power Electronics* 17, no. 5 (Sep 2002): 779-87, doi:10.1109/TPEL.2002.802183
8. Bose, B., Simoes, M., Crecelius, D., Rajashekar, K. et al., "Speed Sensorless Hybrid Vector Controlled Induction Motor Drive," *Ias '95 - Conference Record of the 1995 Ieee Industry Applications Conference/Thirtieth Ias Annual Meeting, Vols 1-3* (1995): 137-43, doi: 10.1109/IAS.1995.530294
9. Instruments T. TMS320F28335, Digital Signal Controllers (DSCs), Data Manual, Literature Number: SPRS439I, 2007.
10. Akin, B. and Bhardwaj, M. "Sensored Field Oriented Control of 3-phase Induction Motors," Texas Instrument Guide, 2013
11. Instruments, Texas, TMS320x2833x, 2823x enhanced pulse width modulator (ePWM) module reference guide (literature number: SPRUG04A). 2009.
12. Men, X., Guo, Y., Wu, G., Shi, C. et al., "Implementation of a Motor Control System for Electric Bus Based on DSP." Paper presented at the 20th International Conference on Electrical Machines and Systems, ICEMS 2017, August 11, 2017 - August 14, 2017, Sydney, NSW, Australia, 2017, doi:2017.10.1109/icems.2017.8056504.
13. Khan, A. and Kress, M., "Identification of Permanent Magnet Synchronous Motor Parameters," SAE Technical Paper 2017-01-1237, 2017, doi:10.4271/2017-01-1237.

## Contact Information

Xiaojin Men

xjmen@mail.ustc.edu.cn

Affiliations:

1. University of Science and Technology of China (USTC)
2. China Automotive Technology and Research Centre (CATARC)